Photochemical & Photobiological Sciences

Accepted Manuscript

This is an *Accepted Manuscript*, which has been through the Royal Society of Chemistry peer review process and has been accepted for publication.

Accepted Manuscripts are published online shortly after acceptance, before technical editing, formatting and proof reading. Using this free service, authors can make their results available to the community, in citable form, before we publish the edited article. We will replace this *Accepted Manuscript* with the edited and formatted *Advance Article* as soon as it is available.

You can find more information about *Accepted Manuscripts* in the Information for Authors.

Please note that technical editing may introduce minor changes to the text and/or graphics, which may alter content. The journal's standard Terms & Conditions and the Ethical guidelines still apply. In no event shall the Royal Society of Chemistry be held responsible for any errors or omissions in this *Accepted Manuscript* or any consequences arising from the use of any information it contains.

ROYAL SOCIETY OF CHEMISTRY

www.rsc.org/pps

Photochemical & Photobiological Sciences

ARTICLE

A simple and sensitive flow injection method based on catalytic activity of CdS quantum dots in acidic permanganate chemiluminescence system for determination of formaldehyde in water and wastewater

Received 00th January 20xx,
Accepted 00th January 20xx

DOI: 10.1039/x0xx00000x

www.rsc.org/

Alireza Khataee,*[a] Roya Lotfi,[a] Aliyeh Hasanzadeh,[a] Mortaza Iranifam[b]

A simple and sensitive flow injection chemiluminescence (CL) method in which CdS quantum dots (QDs) enhanced the CL intensity of $KMnO_4$-formaldehyde (HCHO) reaction was offered for determination of HCHO. This CL system was based on catalytic activity of CdS QDs and its participation in CL resonance energy transfer (CRET) phenomenon. A possible mechanism for the supplied CL system was proposed by using the kinetic curves of the CL systems and the spectra of CL, photoluminescence (PL) and ultraviolet-visible (UV–Vis). The emanated CL intensity of the $KMnO_4$-CdS QDs system was amplified in the presence of a trace level of HCHO. Based on this enhancement effect, a simple and sensitive flow injection CL method was suggested for determination of HCHO concentration in environmental water and wastewater samples. Under selected optimized experimental conditions, the increased CL intensity was proportional to the HCHO concentration in the range of 0.03 - 4.5 μg L^{-1} and 4.5 - 10.0 μg L^{-1}. The detection limit (3σ) were 0.0003 μg L^{-1} and 1.2 μg L^{-1}. The relative standard deviations (RSD%) for eleven replicate determination of 4.0 μg L^{-1} HCHO were 2.2%. Furthermore, the feasibility of the developed method was investigated via the determination of HCHO concentration in environmental water and wastewater samples.

Keywords: CdS quantum dots; Chemiluminescence; Formaldehyde; Flow injection.

1. Introduction

Formaldehyde (HCHO) is the simplest member of aldehyde family with pungent odour synthesized in 1885.[1, 2] This organic compound is extensively applied in some industries as preserving, disinfectant and bleaching agents. Materials consisting of HCHO which was employed as coating, resin, adhesive, and furniture were converted to significant contaminants.[3] HCHO has perilous effect on human health and may cause health problem such as eye irritation, blindness, asthma attack, headaches, insomnia, nervous system harm, lung cancer, nausea, and allergic skin reactions.[4, 5] In addition, HCHO is released to atmosphere via automobile exhaust gases, photooxidation of methane, other hydrocarbons and household tools. Moreover, a substantial source of HCHO resulting in existing of this substance in aquatic systems is atmospheric deposition.[6] Furthermore, drinking water was contaminated by HCHO through discharge of industrial wastes and oxidative water treatment procedures such as ozonation and chlorination.[7] Aforementioned hazardous effect of HCHO on human health should be enough to merit great attention from scientists. So, attempt to explore a sensitive method for determination of HCHO in water samples has substantial importance. On the other hand, HCHO is a substance widely uses in different industries and discharge of industrial wastewater is a great contaminating. So, extraction and determination of HCHO in wastewaters is valuable.[8]

Regarding to comprehensive literature surveys, some analytical methods have been implemented for determination of HCHO in different real samples, including high performance liquid chromatography (HPLC),[2, 9-12] gas chromatography-mass spectrometry (GC-MS),[4] spectrophotometry,[7, 13-15] fluorimetery,[16-19] and chemiluminescence (CL).[6, 20-23]

Among the above stated approaches, CL which has stirred extraordinary attention is considered as a desirable class of detection procedure proposing high sensitivity, high throughput, wide dynamic range and low detection limit for many categories of substances. Moreover, CL procedure provides superiority such as low-cost, rapidity, and no excitation light necessity.[24-26] Since the associated processes in CL systems are rapid, precision and sensitivity of CL depend on the ability of mixing the solutions.[27] Hence, implementation of flow analysis with CL methods improves sensitivity and precision of achieved outputs by affording the fast and reproducible mixing of reagents in the proximity of detector.[28]

Recently, most researchers' attempts have been concentrated on improving the analytical attributes of conventional CL methods by employing nanomaterials which intensify signals and enhance sensitivity and stability of conventional CL systems.[25, 29, 30] It is worthy to mention that attractive characteristics of nanomaterials such as unique size and physicochemical attributes take part in CL system improvement.[25, 31] Quantum dots (QDs) owning

[a] *Research Laboratory of Advanced Water and Wastewater Treatment Processes, Department of Applied Chemistry, Faculty of Chemistry, University of Tabriz, 51666-16471 Tabriz, Iran*
[b] *Department of Chemistry, Faculty of Science, University of Maragheh, 55181-83111 Maragheh, Iran*
* *Corresponding author*
E–mail address: a_khataee@tabrizu.ac.ir (ar_khataee@yahoo.com)
Tel.: +98 41 33393165; Fax: +98 41 33340191

extraordinary optical and electronic properties have captured remarkable consideration of researchers in view of broad utilizations in diverse areas of bio-labelling, bio-imaging, and multicoloured photoluminescent probes.[32-34] So, employing of QDs in CL system is a good strategy for overcoming the low quantum yield deficiency of some CL systems.[34, 35]

In the present work, water dispersible L-cysteine capped CdS QDs were prepared via a facile hydrothermal procedure. It was found that CL emission of HCHO and $KMnO_4$ reaction considerably increases by exploiting CdS QDs. Also, further investigation indicated that there is linear relationship between enhancement in the CL intensity and HCHO concentration. Therefore, a facile, simple and sensitive flow-injection CL was offered for determination of HCHO in different water and wastewater samples. In the following experiments, the probable mechanism of the represented CL system using CL, ultraviolet-visible (UV–Vis) absorption and photoluminescence (PL) spectra was investigated.

2. Experimental

2.1. Materials and solutions

Chemicals and reagents employed through the experiments were of analytical grade and purchased from Merck Co. (Germany). Deionized water was applied during the whole experiments. Preparation of 100 mg L^{-1} HCHO stock standard solution was performed by diluting 250 µL of 37 % HCHO solution to 1 L with deionized water.

2.2. Apparatus

The emitted CL signals during the involving CL reactions in the flow cell were measured using a FB12 luminometer (Berthold detection systems, Germany). Data processing was accomplished by the coupled computer. Scanning the UV-Vis spectrum of the samples was performed by UV-Vis spectrophotometer (S2000, WPA Lightwave, England). Crystal structure investigation of as-synthesized CdS QDs sample was acquired by powder X-ray diffraction (XRD) analysis conducted utilizing a Siemens X-ray diffraction D5000 diffractometer (California, USA), comprised of Cu Kα radiation source (1.54065 Å) generated at 40 kV and 35 mA at room temperature. The mean crystalline size of the as-prepared samples was evaluated using the Debye-Scherrer expression.[36] The Scanning electron microscopy (SEM) image which applied for morphological and structural feature investigation of as-prepared samples was scanned with Mira3 FEG (Tescan, Czech Republic). Moreover, further investigation about the diameter size of as-prepared nanoparticles was performed via Microstructural Image Processing (MIP) software (Nahamin Pardazan Asia Co., Iran). Fourier transform infrared (FT-IR) spectra were taken with KBr pellets by applying of IR-spectrometer (Tensor 27, Bruker, Germany). The PL spectra were acquired with a spectrofluorometer (FP-6200, Jasco, Japan). CL spectra were recorded by a spectrofluorometer in which the xenon lamp was turned off.

2.3. Procedures for chemiluminescence assay

The CL pattern was analyzed using lab-made flow injection CL detection system represented in Figure S1. The proposed device composes of a peristaltic pump, four lines, and a six-port injection valve with 150 µL loop. All flow lines were polytetrafluoroethylene (PTFE) tubes (1.0 mm internal diameter (i.d.)). As indicated in Figure S1, the solution of acid (line (a)), sample or standard solution of the mixture of HCHO and CdS QDs (line (b)), deionized water as the carrier (line (c)), and $KMnO_4$ solution (line (d)) were propelled with flow rate set at 2.0 mL min^{-1} via peristaltic pump. The merged solution of lines (a) and (b) via passing mixing tube (silicon tubing, 1.0 mm i.d.) was delivered to the stream of carrier and combined with the flow of the $KMnO_4$ solution through a Y-piece. After introducing the mentioned combined streams into the flow cell, CL emission was initiated. Obtained signals through connected computer were processed via software provided by the manufacturer of the luminometer. The determination of HCHO was relied on the enhancement effect of HCHO on CL intensity obtained according to the formula: $\Delta I = I_s - I_0$, where I_s and I_0 were the CL intensity in the presence and absence HCHO, respectively.

2.4. Synthesis of L-cysteine capped CdS QDs

Synthesis of water-dispersed CdS QDs was accomplished via hydrothermal method following portrayed approach in our former works.[26, 37] Concisely, $Cd(CH_3COO)_2.2H_2O/Na_2S$ with defined molar proportion of 1:1.7 were dissolved in 30 mL of distilled water and regulating the pH value of obtained solution was accomplished using 1.0 M NaOH solution. L-cysteine solution was blended with the above-noted mixture so that the final molar proportion of Cd^{2+}/S^{2-}/L-cysteine was kept at 1:1.7:2.3 in the achieved solution. The obtained solution was undergone deaeration via bubbling under nitrogen for 30 min and transmitted into a 100 mL Teflon-lined stainless steel autoclave. After completing the heating step of seal autoclave in an oven and at 150 °C for defined times (4, 5, and 6 h), the autoclave was cooled to room temperature. Absolute ethanol was employed for acquiring the better precipitation of as-prepared L-cysteine capped CdS QDs. Afterward, the accumulated samples were washed with deionized water and absolute ethanol several times to eliminate the remainder reactants and maintained in air-dry at room temperature for 2 h.

2.5. Pre-treatment of real sample solutions before assay

Tap water, underground water and wastewater samples were newly accumulated into pre-cleaned polyethylene flasks according to standard methods[29] and selected for following analysis. Eliminations of solid contamination from water samples were accomplished by filtration through a 0.45 µm pore size polyamide membrane filter according to standard methods.

In the case of tap water and underground water samples, prior to the determination analysis, the obtained water samples were spiked with HCHO from its stock solution in order to make solutions with 0.3, 0.5, 2.0, and 4.0 µg L^{-1} concentrations. Removing interferences of metal cations in determination of HCHO in environmental samples was performed by passing through a packed exchange column with the strong cation-exchanging resin (Chelex 100) at a flow rate of 4 mL min^{-1}. The prepared solutions were employed for the determination of HCHO concentration relying on the general procedure. Finally, the same approach was exploited for blank sample, without HCHO, for the determination of the blank value.

For determination of HCHO in wastewater of paint factory in Tabriz, Iran, HCHO extraction was accomplished according to literature.[8] In this sense, the obtained filtrated sample was passed through a packed exchange column with the strong cation-exchanging resin (Chelex 100) at a flow rate of 4 mL min^{-1}. pH of 10 mL of sample solution containing the HCHO, 0.05 mol L^{-1} of methyl acetoacetate as derivatization agent, and 20% (w/v) of NaCl was adjusted at 6.4 in a glass test tube with conic bottom. The blended solution was remained at 60 °C for 10 minutes and cooled down in water for 5 min. In the next step, 1.0 mL methanol (dispersive solvent) comprising 75 µL ionic liquid $[C_6MIM][PF_6]$ was injected by 1.0 mL syringe, rapidly. After centrifuging for 5 min at 3,000 rpm, cloudy solution was used for the following analysis.

Photochemical & Photobiological Sciences ARTICLE

Before the determination analysis, 500 µL of the obtained wastewater sample were dispersed in 300 µL methanol and diluted with deionized water. Furthermore, wastewater samples were spiked with HCHO from its stock solution in order to make solutions with 0.4 and 1 µg L^{-1} concentrations.

3. Results and discussion

3.1. Optical characteristics of synthesized CdS QDs

Optical characteristic assessment of CdS QDs which were formed in three various heating times (4, 5, and 6 h) was conducted by utilization of the room temperature UV-Vis absorption and PL spectra represented in Figures 1a and 1b, respectively.

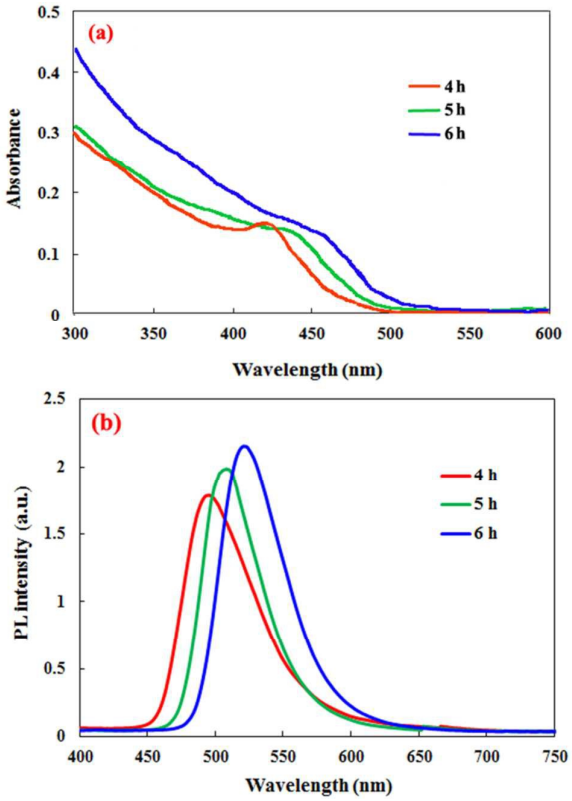

Figure 1. *(a): UV-Vis absorption and (b): PL spectra of CdS QDs after different synthesis times (4, 5, and 6 h) at 150 °C. CdS QDs concentration: 1.0 mmol L^{-1}; excitation wavelength: 375 nm.*

As indicated in the figure, red shift to longer wavelength in absorption spectra which attributes to the first exciton peak (1_{sh}-1_{se}) arises from nanocrystal growth during hydrothermal process.[38, 39] The achieved results are in accordance with former investigations proving quantum confinement in the synthesized CdS QDs. Peng's equation[40] was applied to estimation of the as-prepared CdS QDs diameter as follow:

$$D = (-6.6521 \times 10^{-8})\lambda^3 + (1.9557 \times 10^{-4})\lambda^2 - (9.2352 \times 10^{-2})\lambda + 13.29 \quad (1)$$

In the aforementioned formula, D (nm) and λ (nm) express estimated size of CdS QDs and the wavelength of the first excitonic absorption peak of the QDs, respectively. Obtained results from diameter determination of CdS QDs via the noticed expression indicated that diameter of nanocrystals treated with 4, 5, and 6 h hydrothermal procedure were 4.07, 4.85 and 5.32 nm, respectively. In view of the fact that QDs band gap (E_g) is a significant point in the associated CL reaction, evaluation of the optical direct band gap energy of as-prepared CdS QDs was performed using the UV-Vis absorption spectra of CdS QDs samples and Tauc's equation:[41]

$$(Ahν)^2 = K(hν–E_g) \quad (2)$$

In the noted equation, A, hυ, K and E_g are representative of the absorption coefficient, the photon energy (eV), a constant and the optical direct band gap, respectively.

The band gap energy of the CdS QDs with 4, 5, and 6 h heating times relying on the extrapolation of linear portion graph of $(Ahν)^2$ versus hν were evaluated as 2.96, 2.83, and 2.62 eV, respectively.

Complementary studies confirm quantum confinement in all synthesized CdS QDs samples based on gained E_g of synthesized CdS QDs which are higher than the described value for bulk CdS with absorption onset at 515 nm (E_g = 2.42 eV).[40] Moreover reduce in E_g of QDs which results from growth in nanocrystals size can be assigned to the quantum confinement effect in all as-prepared samples.[42]

3.2. Structural characteristics of synthesized CdS QDs

Crystalline feature investigation of CdS QDs was performed using X-ray diffraction (XRD) pattern of L-cysteine capped CdS QDs. XRD pattern of CdS QDs which underwent 6 h hydrothermal heating process was represented in Figure 2a. As obviously evident in the figure, main XRD diffraction peaks of the L-cysteine capped CdS QDs situating at 2θ (scattering angle) values of 24.9°, 26.6°, 28.3°, 36.8°, 43.9°, 48.1°, 52.1°, 58.6°, and 67.1° can ascribe to the (100), (002), (101), (102), (110), (103), (112), (202), and (203) plane reflections. These results verify that synthesized CdS QDs are in accordance with the standard patterns of hexagonal wurtzite CdS (JCPDS 41-1049).[43, 44] Furthermore, as displayed in the figure, synthesized QDs have high purity. The mean crystalline size of CdS QDs formed at 6 h hydrothermal was assessed to be about 5 nm by exploiting the Debye–Scherrer formula[36] and the sharpest peak of XRD plan (2θ of 28.3°).

Further evaluation about the morphology and particle size of as-prepared CdS QDs was performed via the study of SEM image of CdS QDs prepared at 6 h hydrothermal duration (Figure 2b). Spherical-like shape and well homogeneity of synthesized CdS QDs are evident from the image. Also, CdS QDs size frequency investigation was carried out by employing MIP software.[45-47] Investigations indicated that average particle size is 5-9 nm (Figure 2c), which is in a good accordance with the XRD and optical outcomes.

L-cysteine attachment on the surface of CdS QDs was distinguished using investigation of FT-IR spectra of free L-cysteine and L-cysteine capped CdS QDs samples (Figure S2). Regarding the two mentioned spectra comparison, disappearing of thiol group stretching peak (2550 to 2670 cm^{-1}) in the FT-IR spectrum of L-cysteine capped CdS QDs arises from bonding of the thiol group of L-cysteine to CdS QDs surface implying presence of L-cysteine on the surface of CdS QDs.[48, 49]

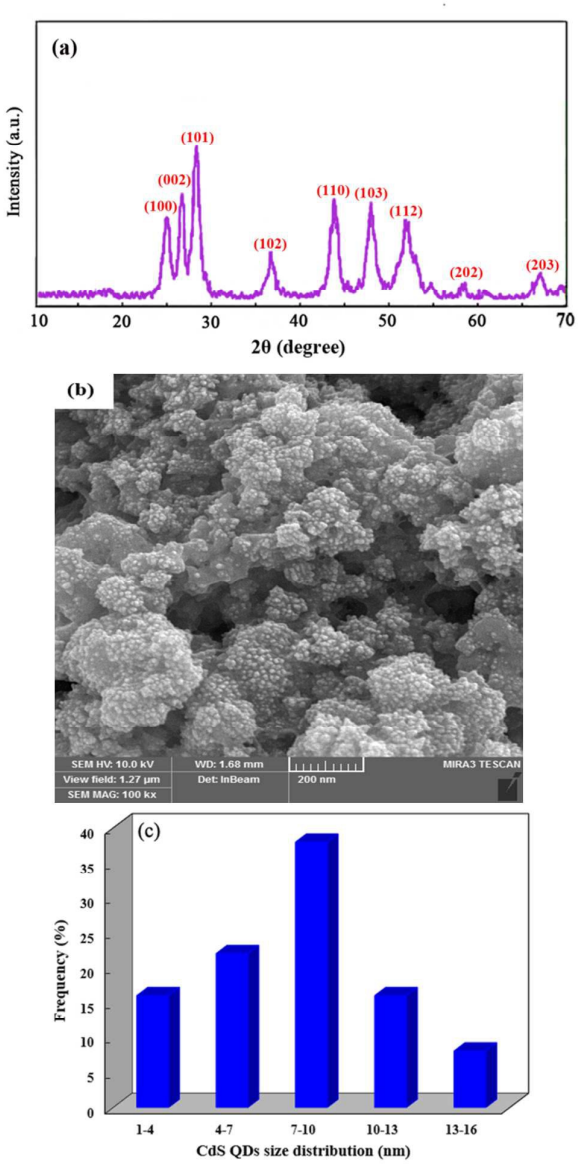

Figure 2. *(a): XRD pattern, (b): SEM and (c): particle size distribution of L-cysteine capped CdS QDs.*

3.3. Chemiluminescence reaction enhanced by CdS QDs

The kinetic curves of CL system are exhibited in Figure 3. Preceding evaluations revealed that CL emission generated upon reaction of HCHO and $KMnO_4$ (see Figure 3, curve a). In addition, investigations in this work indicated that CdS QDs considerably amplify the CL intensity emanated from $KMnO_4$-HCHO reaction (see Figure 3, curve c). Results of further experiments reveal that $KMnO_4$ in acidic media is capable of inducing a CL emission from CdS QDs (see Figure 3, curve b). As is recognizable from the figure, the produced CL signals from $KMnO_4$-HCHO and $KMnO_4$-CdS QDs reactions are so weak in comparison with $KMnO_4$-HCHO-CdS QDs CL signals. Controlling assessments were accomplished using the reagents applied for the synthesis of CdS QDs ($Cd(CH_3COO)_2$, L-cysteine, and Na_2S solutions). The mentioned reagents have no effect on the CL emission. The achieved results confirm that amplification in the CL intensity arises from association of CdS QDs. The CL intensity of $KMnO_4$-HCHO (6.1 μg L^{-1})-CdS QDs system is about 35 times greater than CL intensity in the absence of CdS QDs. Furthermore, it is completely obvious that CL reaction of $KMnO_4$-HCHO in the presence of CdS QDs is comparatively fast. This statement proves the accelerating effect of CdS QDs on the mentioned CL reaction, which ascribes to the catalytic performance of CdS QDs. As shown in Figure 3, curve d and e, when concentration of HCHO was increased, CL signal intensity could considerably intensify. These observations declare that the proposed CL system can be developed as the simple and sensitive method for the determination of HCHO.

Also, the effect of other aldehydes such as acetaldehyde, propionaldehyde, butyraldehyde, benzaldehyde, glyoxal and glutaraldehyde on the $KMnO_4$-CdS QDs CL system was investigated. The relative CL intensity of $KMnO_4$-CdS QDs in the presence of acetaldehyde, propionaldehyde, butyraldehyde and benzaldehyde was shown in Figure S3. The effect of the aldehydes in comparison with the effect of HCHO on $KMnO_4$-CdS QDs CL system is negligible. Furthermore, the relative CL intensity of $KMnO_4$-CdS QDs system in the presence of 0.4 mg L^{-1} of glyoxal and glutaraldehyde was studied and shown in Figure S4. Increase in the intensity of CL emission of $KMnO_4$-CdS QDs system in the presence of glyoxal and glutaraldehyde is considerable in comparison with the other aldehydes. It can be mentioned that trace amounts of HCHO can intensively enhance the intensity of the $KMnO_4$-CdS QDs CL system in which the increased CL intensity was proportional to the HCHO concentration. Furthermore, according to Jacqui et al. [50], low molecular weight aldehyde can be employed as enhancer in permanganate CL system. In this context, the results of our investigations about the effect of other aldehydes on $KMnO_4$-CdS QDs CL system are in accordance with those reported in the literature.[51,52].

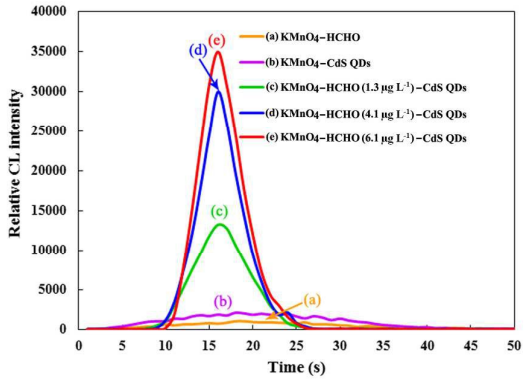

Figure 3. *Kinetic curves for (a): $KMnO_4$–HCHO (b): $KMnO_4$–CdS QDs and (c), (d), (e): $KMnO_4$–HCHO–CdS QDs CL system with different concentration of HCHO. The concentrations of $KMnO_4$, HCl, CdS QDs were 0.06 mmol L^{-1}, 1.0 mol L^{-1}, 0.7 mmol $L^{-1}$and concentration of HCHO in (a), (c), (d) and (e) were 30.0 μg L^{-1}, 1.3 μg L^{-1}, 4.1 μg L^{-1} and 6.1 μg L^{-1}, respectively.*

Complementary investigation reveals that sodium hexametaphosphate (SHMP) can increase CL signal of CdS QDs-$KMnO_4$ which is shown in Figure 4. But, increase in CL intensity of CdS QDs-$KMnO_4$ in the presence of SHMP is low in compare with CL intensity in the presence of HCHO (Figure 4). Since the increase in the signal of $KMnO_4$-SHMP-CdS QDs CL system in the presence of different concentrations of HCHO is not proportional to HCHO concentration, this CL system seems to not be proper for sensitive determination of trace HCHO.

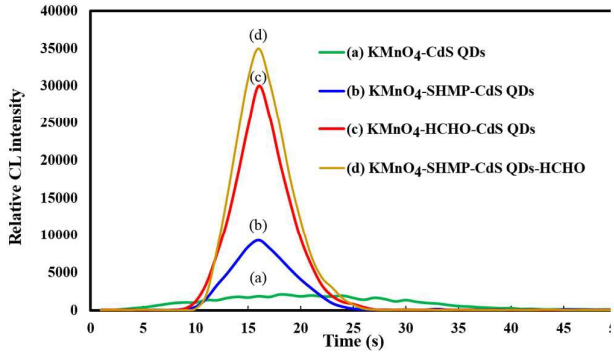

Figure 4. *Kinetic curves for (a): $KMnO_4$–HCHO (b): $KMnO_4$–SHMP–CdS QDs (c): $KMnO_4$–HCHO–CdS QDs and (d): $KMnO_4$–SHMP–CdS QDs–HCHO CL system with different concentration of HCHO. The concentrations of $KMnO_4$, HCl, CdS QDs, HCHO in (c) and (d), and SHMP were 0.06 mmol L^{-1}, 1.0 mol L^{-1}, 0.7 mmol L^{-1}, 0.5 mmol L^{-1}, 6.1 μg L^{-1}, and 4 mmol L^{-1}, respectively.*

3.4. Optimization of the chemiluminescence reaction conditions

A series of evaluations concerning to the impact of $KMnO_4$ concentration, various types and concentration of acid, particle size and concentration of CdS QDs on emitted CL signal was developed. In this context, impact of different concentrations of $KMnO_4$ in the range of 0.01-0.8 mmol L^{-1} on the CL signals was assessed (see Figure S5a). According to the figure, the highest CL signal was generated at 0.06 mmol L^{-1} concentration of $KMnO_4$. Further increase in $KMnO_4$ concentration more than 0.06 mmol L^{-1} gives rise to decrease trend which can be assigned to potential non-radiative de-excitation.[50] So, 0.06 mmol L^{-1} of $KMnO_4$ was selected for the following analysis.

Type and concentration of acid have influence on permanganate involved CL reaction.[50] In the following step, effect of HCl, HNO_3, H_3PO_4 and HNO_3 over the range of 0.01-2.0 mol L^{-1} was evaluated and shown in Figure S5b. According to the figure, the CL intensity in HCL medium with 1.0 mol L^{-1} concentration was achieved to the highest value. Therefore, 1.0 mol L^{-1} of HCL was selected for subsequent analysis.

In order to study the impact of particle size of CdS QDs on induced CL intensity, CdS QDs with particle size of 4.07 to 5.32 nm was employed in CL system. The result of analysis revealed that increase in particle size of CdS QDs follows enhancement in CL emission. The mentioned observation can be attribute to the facilitation in process of electron injection to the CdS QDs arising from reduce in E_g of QDs with an increase in particle size according to the CL energy match theory.[39, 53]

Ultimately, concentration effect of CdS QDs with appropriate particle size of 5.32 on the intensity of CL emission was investigated. As is apparent from Figure S5c, 0.7 mmol L^{-1} of CdS QDs induce the highest CL emission and subsequent increase in CdS QDs concentration leads to weakness in the CL intensity. In this matter, it can be mentioned that high concentration of CdS QDs causes intense interaction.[32, 53] Therefore, 0.7 mmol L^{-1} of CdS QDs was used as optimized value.

3.5. Possible chemiluminescence mechanism

Investigation of emitting species relating to the CL system is important point in clarifying the probable mechanism. Hence, CL, PL, and UV–Vis analysis were implemented. The obtained CL spectra were used for discovering the emitting species and function of CdS QDs in $KMnO_4$–HCHO–CdS QDs CL reaction. As demonstrated in Figure 5, curve a, HCHO was oxidized by $KMnO_4$ in acidic media leading to generation of CL emission. Regarding the extensive bibliography surveys, Mn (III) generated through reduction process of permanganate with aldehyde. Mn (III) species can be maintained in the solution in the presence of a stabilizing agent such as polyphosphate. Moreover, further reduction reaction of Mn (III) can be accomplished by aldehyde and in the absence of stabling agent, which produces $Mn(II)^*$. On the other hand, nucleophilic addition of permanganate to aldehydes gives rise to formation of permanganate ester intermediate.[54, 55] According to the figure, emitted CL signal of $KMnO_4$-HCHO which was in the range of 450 to 650 nm can be assigned to the generated permanganate ester intermediate, during oxidation of HCHO according to literature investigations.[20] Oxidation of HCHO by $KMnO_4$ can be demonstrated as follow:

$$MnO_4^- + 2\,HCHO + 4\,H^+ \rightarrow 2\,HCOOH + Mn(III) + 2\,H_2O + h\upsilon\ (\lambda_{em} = 450 - 650\ nm) \quad (3)$$

$$2\,Mn(III) + HCHO + H_2O \rightarrow HCOOH + 2\,Mn\,(II)^* + 2\,H^* \quad (4)$$

$$Mn\,(II)^* \rightarrow Mn\,(II) + h\upsilon\ (\lambda_{max} \cong 725\ nm) \quad (5)$$

As revealed in the Figure 5, curve c, CL emission of $KMnO_4$-HCHO in the presence of CdS significantly is increased. In this sense, it should be mentioned that the oxidative decomposition of permanganate ester intermediate generated through the nucleophilic addition of permanganate to HCHO is the rate-determining stage in the oxidation process.[54, 55] It can be supposed that CdS QDs accelerate oxidative decomposition of permanganate ester intermediate.

In addition, CL emission through the reaction of CdS QDs with $KMnO_4$ in acidic condition in the range of 500–600 nm (Figure 5, curve b) matching with PL spectrum of CdS QDs with 5.32 nm particle size (Figure 1b) can be attributed to the formation of $(CdS\ QDs)^*$. According to preliminary investigation, hole injection process can be achieved along oxidation of CdS QDs with $KMnO_4$. In this sense, excitation of electrons into the high energy levels can perform at temperatures higher than absolute zero.[56] Coinciding of the two aforementioned process leads to exciton formation. Consequently, CL response induces over the returning of excited state of CdS QDs ($(CdS\ QDs)^*$) to its ground state are clearly illustrated in the consequent expressions:

$$MnO_4^- + CdS\ QDs + 8H^+ \rightarrow Mn\,(II)^+ + (CdS\ QDs)^* + 4H_2O \quad (6)$$

$$(CdS\ QDs)^* \rightarrow CdS\,QDs + h\upsilon\,(\lambda_{max} \cong 520\,nm) \quad (7)$$

As is clearly evident from the Figure 5, curve c, CL signals of $KMnO_4$-HCHO considerably increase by participation of CdS QDs. In this case, it also can be mentioned that broad absorption band of CdS QDs with particle size of 5.32 nm (see Figure 1a) overlaps with emission band of HCHO. Therefore, it can be proposed that CdS QDs can behave as sensitizers which enhance CL intensity of $KMnO_4$-HCHO reaction with association in CL resonance energy transfer (CRET) procedure from the mentioned redox reaction.

As is clear in Figure 5, curves a, b, and c, the second peak is located around 725 nm. According to complementary literature review, participation of permanganate in acidic condition CL reaction emanate radiation with a maximum wavelength near 734 ± 5 nm can be allotted to the excited Mn(II) ($Mn(II)^*$) (from the $^4T_1$ to $^6A_1$ transition) in the acidic permanganate CL systems [50] simplified as follow:

$$Mn(II)^* \rightarrow Mn(II) + h\upsilon\ (\lambda_{max} \cong 725nm) \quad (9)$$

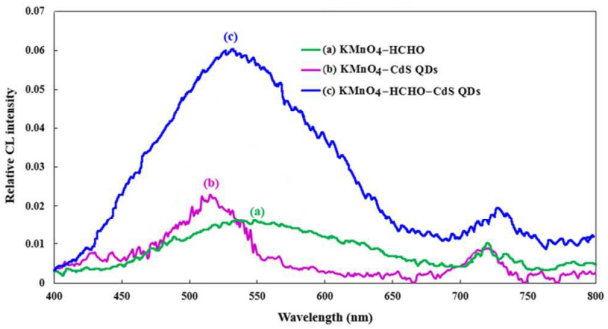

Figure 5. *CL spectra of (a): $KMnO_4$–HCHO (b): $KMnO_4$–CdS QDs and (c): $KMnO_4$–HCHO–CdS QDs CL system. The concentrations of $KMnO_4$, HCHO in (a) and (c), HCl, and CdS QDs were 0.06 mmol L^{-1}, 25.0 µg L^{-1} and 6.5 µg L^{-1}, 1.0 mol L^{-1}, and 0.7 mmol L^{-1}, respectively.*

Moreover, Figures 5a and 5b demonstrate the UV–Vis absorption spectra of the $KMnO_4$-HCHO CL system in the absence and presence of CdS QDs, respectively.

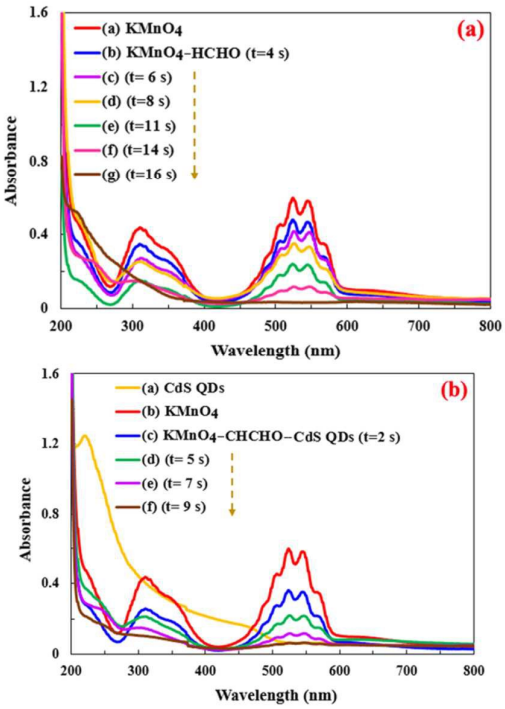

Figure 6. *UV–Vis absorption spectra of (a): $KMnO_4$–HCHO CL system and (b): $KMnO_4$–HCHO–CdS QDs in acidic media, recorded at different time intervals after their mixing. Conditions: the concentrations of $KMnO_4$, HCHO, CdS QDs, and HCl were 0.06 mmol L^{-1}, 8.5 µg L^{-1}, 0.7 mmol L^{-1}, and 1.0 mol L^{-1}, respectively.*

As represented in Figure 6b, UV–Vis absorption spectrum of $KMnO_4$–HCHO–CdS QDs CL system, decline in absorption band of $KMnO_4$ is faster than decline in absorption band of $KMnO_4$ in Figure 6a, UV–Vis absorption spectrum of $KMnO_4$-HCHO CL system in the absence of CdS QDs. It implies that CdS QDs facilitate consumption of $KMnO_4$ in the reaction resulting from catalytic function of CdS QDs.

3.6. Analytical performance for HCHO determination

Under the optimum conditions, the enhancement effect of HCHO on the suggested CL intensity is linear over the concentration range of 0.03 - 4.5 µg L^{-1} and 4.5 - 10.0 µg L^{-1}. The linear regression equation is y= 6169.6 x + 3985.2 (r^2 = 0.99), where y is I, and x is the HCHO concentration in µg L^{-1}. The limit of detection (LOD) (3σ) of the developed CL method was calculated to be 0.0003 µg L^{-1} and 1.2 µg L^{-1}. Also, the limit of quantification (LOQ) of the developed CL method was calculated to be 0.001 µg L^{-1}.The relative standard deviation (RSD%) is 2.18% for eleven replicate determinations of 4.0 µg L^{-1} HCHO. These outcomes reveal that the offered CL system has relatively high sensitivity, a good linear range, and desirable precision. Furthermore, some investigated methods for determination of HCHO in literature were compared with the developed CL system (see Table 1). The developed CL method possessing advantages such as rapidity, simplicity, relatively inexpensive configuration, and high sensitivity improves linear range and LOD of the previously reported CL method.[6, 20-23]

Table 1. A comparison of different analytical techniques for the determination of HCHO.

Method	Matrix	LR[a] (µg L^{-1})	LOD (µg L^{-1})	Ref.
HPLC [a]	Beer Samples	46-4600	16	2
Fluorimetery	Resin and the air of an animal specimens room	40–1190	7.5	19
Spectrophotometry	Chemical industrial wastewater and phenol formaldehyde resin	14-700	7	13
	Formulations and biological fluids	470-40000	360	14
	Fabric and air	1000-20000	20	15
CL	Textiles	0.606-3.03	1.51	21
	Indoor air	0.06–3.0	0.01	20
CL	Environmental waters samples	0.03-4.5 4.5-10.0	0.0003 and 0.0009	This work

a Linear range

b High performance liquid chromatography

3.7. Interference study

With a view to evaluate the potential application of the noted CL method for measurement of HCHO in real sample, the selectivity of the method for determination of HCHO in the presence of interfering foreign species need to be investigated. In this sense, determination of HCHO in solution involving 5.0 µg L^{-1} HCHO and diverse value of potentially interfering compounds was performed. The outcomes for external compound values resulting in a relative error of less than 5% in the CL intensity were distinguished as the tolerance limit of each compound in the determination of HCHO explained in Table S1. Metal ions interference elimination regarding Table S1 was accomplished by passing the real sample mixture through a packed strong cation exchanger column. Furthermore, the effect of phenols like quercetin, rutin, gallic acid and vanillin on the CL emission of $KMnO_4$-CdS QDs system was investigated. Although extraction method exhibits good selectivity for HCHO and eliminated the interfering effect of phenolic compounds and other interferences,[8] tolerable concentration ratios of phenolic compounds with respect to 5.0 µg L^{-1} of HCHO were added in Table S1. The results reveal that the above mentioned phenols have enhancing effect on $KMnO_4$-CdS QDs CL system. Furthermore, the relative CL intensity of $KMnO_4$-CdS QDs in the presence of quercetin, rutin, gallic acid and vanillin was shown in the Figure S6. So, this problem was solved by extraction of HCHO from real samples. It should be mentioned that enhancing effect of trace concentrations of HCHO (6.1 µg L^{-1}) on the

$KMnO_4$-CdS QDs CL system (relative CL intensity~30000) is considerable in comparison with increase in CL emission in the presence of the noted phenolic compounds (5.0 mg L^{-1}) (Figure S6). Therefore, developed CL approach can be considered a selective method for determination of HCHO in environmental water and wastewater samples.

3.9. Analytical application study

In order to verify the practical application of the proposed CL method, the mentioned approach was exploited for determination of HCHO in tap water, underground water and wastewater samples. The real samples were provided for analysis as hinted approach in the Section 2.5. The achieved consequence eventuating from the evaluation of HCHO contents in the spiked environmental water and wastewater samples by a standard addition method are portrayed in Tables 2 and Tables 3, respectively. The percentage recovery tests were accomplished to investigate the veracity and efficiency of the induced CL system. Moreover, for validation of the proposed CL method a fluorimetric method[57] as an official method was applied for determination of HCHO. The obtained results were summarized in Table 4 prove the good agreement of results acquired by proposed CL method with those obtained by fluorimetric method. The data was evaluated by Student t-test (p=0.05), which shows that results are not significantly different. The received outcomes reveal that mentioned CL approach supply good precision for the potential application of this method for the determination of HCHO in real samples**.**

Table 2. Obtained results for the determination of HCHO in spiked water samples.

Sample	Added (μg L^{-1})	Found [a] (μg L^{-1})	Recovery (%)
Tap water	0	Not detected	-
	0.3	0.31±0.03	103.89
	2.0	2.12±0.3	105.83
Under ground water	0	Not detected	-
	0.5	0.52±0.03	104.0
	4.0	4.15±0.2	103.75

a Mean of six determinations ± standard deviation.

Table 3. Obtained results for the determination of HCHO in spiked wastewater samples.

Sample	Added (μg L^{-1})	Found [a] (μg L^{-1})	Recovery (%)
Wastewater [b]	0	7.62	-
	0.4	8.05±0.05	100.37
	1.0	8.71±0.08	101.04

a Mean of six determinations ± standard deviation.

b Wastewater of paint factory

Table 4. Validation results for the determination of HCHO in spiked water sample.

Sample	Added (μg L^{-1})	Official method [a] (μg L^{-1})	Proposed CL method [a] (μg L^{-1})	t-statistic [b]
Underground water	9.0	9.25±0.53	9.86±1.26	2.91
Drinking water	10.0	10.48±1.67	9.52±1.96	2.15

a Mean of three determinations ± standard deviation.

b *t*-critical=4.30 for n=2and *P*=0.05.

4. Conclusions

In the present paper, CdS QDs enhanced the CL intensity of $KMnO_4$-HCHO reaction regarding to its catalytic function and participation in CRET. Based on the enhancing effect of HCHO on emitted CL intensity, a simple flow–injection CL method was developed for determination of HCHO. Furthermore, it supplies sufficient sensitivity without using an expensive CL reagent. Eventually, the method has been successfully applied to the analysis of HCHO in environmental water and wastewater samples.

Acknowledgments

The authors thank the University of Tabriz (Iran) for all the support provided.

Notes and references

1. T. Salthammer, The formaldehyde dilemma, ***Int J Hyg Environ Health***, 2015, **218**, 433-436.
2. J. Zhao, G. Wang, T. Cao and Z. Guo, Development of a novel derivate assay for formaldehyde determination by HPLC in beer samples, ***Food Anal Mthod***, 2015, **7**, 1-8.
3. T. Salthammer, S. Mentese and R. Marutzky, Formaldehyde in the indoor environment, ***Chem. Rev***, 2010, **110**, 2536-2572.
4. F. A. Lobo, T. M. Santos, K. M. Vieira, V. M. Osorio and J. G. Taylor, Determination of formaldehyde in hair creams by gas chromatography-mass spectrometry, ***Drug Test Anal***, 2015, **7**, 848-852.
5. P. Ma, F. Liang, D. Wang, Q. Yang, Y. Ding, Y. Yu, D. Gao, D. Song and X. Wang, Ultrasensitive determination of formaldehyde in environmental waters and food samples after derivatization and using silver nanoparticle assisted sers, ***Microchim Acta***, 2015, **182**, 863-869.
6. K. Motyka, A. Onjia, P. Mikuska and Z. Vecera, Flow-injection chemiluminescence determination of formaldehyde in water, ***Talanta***, 2007, **71**, 900-905.
7. Q. Li, M. Oshima and S. Motomizu, Flow-injection spectrofluorometric determination of trace amounts of formaldehyde in water after derivatization with acetoacetanilide, ***Talanta***, 2007, **72**, 1675-1680.
8. M. Arvand, E. Bozorgzadeh, S. Shariati and M. A. Zanjanchi, Ionic liquid-based dispersive liquid–liquid microextraction for the determination of formaldehyde in wastewaters and detergents, ***Environ. Monit. Assess***, 2012, **184**, 7597-7605.
9. J. Lawrence and J. Iyengar, The determination of formaldehyde in beer and soft drinks by HPLC of the 2, 4-dinitrophenylhydrazone derivative, ***Int J Environ Anal Chem***, 1983, **15**, 47-52.
10. J. R. Li, J. L. Zhu and L. F. Ye, Determination of formaldehyde in squid by high-performance liquid chromatography, ***Asia Pac J Clin Nutr***, 2007, **16**, 127-130..
11. W. Luo, H. Li, Y. Zhang and C. Y. Ang, Determination of formaldehyde in blood plasma by high-performance liquid chromatography with fluorescence detection, ***J Chromatogr B Biomed Sci Appl***, 2001, **753**, 253-257.
12. I. Ueta, S. Mochizuki, S. Kawakubo, T. Kuwabara, K. Jinno and Y. Saito, A novel miniaturized extraction capillary for determining gaseous formaldehyde by high-performance liquid chromatography, ***Anal. Bioanal. Che***m, 2015, **407**, 899-905.
13. A. Afkhami and M. Rezaei, Sensitive spectrophotometric determination of formaldehyde by inhibition of the malachite green–sulfite reaction, ***Microchem. J***, 1999, **63**, 243-249.
14. A. A. Ensafi and Z. Nazemi, Determination of formaldehyde by its catalytic effect on the oxidation of pyrogallol red by bromate using flow-injection

spectrophotometric detection, ***J. Anal. Chem***, 2007, **62**, 987-991.

15. S. Feng, J. Fan, A. Wang, X. Chen and Z. Hu, Kinetic spectrophotometric determination of formaldehyde in fabric and air by sequential injection analysis, ***Anal. Lett***, 2004, **37**, 2545-2555.
16. F. S. de Oliveira, E. T. Sousa and J. B. de Andrade, A sensitive flow analysis system for the fluorimetric determination of low levels of formaldehyde in alcoholic beverages, ***Talanta***, 2007, **73**, 561-566.
17. S. Girousi, E. Golia, A. Voulgaropoulos and A. Maroulis, Fluorometric determination of formaldehyde, ***Fresenius J. Anal. Chem***, 1997, **358**, 667-668.
18. A. L. Lazrus, K. L. Fong and J. A. Lind, fluorometric determination of formaldehyde in air, ***Anal. Chem***, 1988, **60**, 1074-1078.
19. X. Q. Zhan, D. H. Li, Q. Z. Zhu, H. Zheng and J.-G. Xu, Sensitive fluorimetric determination of formaldehyde by the co-quenching effect of formaldehyde and sulfite on the fluorescence of tetra-substituted amino aluminium phthalocyanine, ***Analyst***, 2000, **125**, 2330-2334.
20. S. Han, J. Wang and S. Jia, Determination of formaldehyde based on the enhancement of the chemiluminescence produced by CdTe quantum dots and hydrogen peroxide, ***Microchim. Acta***, 2014, **181**, 147-153.
21. S. Kanwal, Q. Ma, X. Fu, P. Yuan and X. Su, A flow-injection chemiluminescence determination of formaldehyde in textiles, ***Spectrosc. Lett***, 2010, **43**, 84-90.
22. B. Li, M. Liu, Z. Zhang and C. XU, Flow-injection chemiluminescence determination of formaldehyde with a bromate-rhodamine 6G system, ***Anal. Sci***, 2003, **19**, 1643-1646.
23. Y. Maeda, X. Hu, S. Itou, M. Kitano, N. Takenaka, H. Bandow and M. Munemori, Continuous determination of gaseous formaldehyde by a chemiluminescence method, ***Analyst***, 1994, **119**, 2237-2240.
24. L. P. da Silva and J. C. E. da Silva, Firefly luciferin as a multifunctional chemiluminescence molecule , ***Photochem. Photobiol. Sci***, 2013, **12**, 1615-1621.
25. M. Iranifam, Analytical applications of chemiluminescence-detection systems assisted by magnetic microparticles and nanoparticles, ***TrAC, Trends Anal. Chem***, 2013, **51**, 51-70.
26. A. Khataee, R. Lotfi and A. Hasanzadeh, A novel permanganate–morin–CdS quantum dots flow injection chemiluminescence system for sensitive determination of vancomycin, **RSC Adv**, 2015, **5**, 82645-82653.
27. S. Koronkiewicz and S. Kalinowski, Direct-injection chemiluminescence detector. Properties and potential applications in flow analysis, ***Talanta***, 2015, **133**, 112-119.
28. M. Iranifam, Revisiting flow-chemiluminescence techniques: pharmaceutical analysis, ***Luminescence***, 2013, **28**, 798-820.
29. M. Iranifam, M. Fathinia, T. S. Rad, Y. Hanifehpour, A. Khataee and S. Joo, A novel selenium nanoparticles-enhanced chemiluminescence system for determination of dinitrobutylphenol, ***Talanta***, 2013, **107**, 263-269.
30. A. Khataee, A. Hasanzadeh, R. Lotfi, R. Pourata and S. W. Joo, Determination of dexamethasone by flow-injection chemiluminescence method using capped CdS quantum dots, ***Spectrochim Acta A Mol Biomol Spectrosc***, 2015, **150**, 63-71.
31. A. Khataee, M. Iranifam, M. Fathinia and M. Nikravesh, Flow-injection chemiluminescence determination of cloxacillin in water samples and pharmaceutical preparation by using CuO nanosheets-enhanced luminol–hydrogen peroxide system, ***Spectrochim Acta A Mol Biomol Spectrosc***, 2015, **134**, 210-217.
32. H. Chen, L. Lin, H. Li and J.-M. Lin, Quantum dots-enhanced chemiluminescence: Mechanism and application, ***Coord. Chem. Rev***, 2014, **263**, 86-100.33. S. Dong, W. Guan and C. Lu, *Sensors and Actuators B: Chemical*, 2013, **188**, 597-602.
33. S. Dong, W. Guan and C. Lu, Quantum dots in organo-modified layered double hydroxide framework-improved peroxynitrous acid chemiluminescence for nitrite sensing, ***Sens Actuators B Chem***, 2013, **188**, 597-602.
34. C. Frigerio, D. S. Ribeiro, S. S. M. Rodrigues, V. L. Abreu, J. A. Barbosa, J. A. Prior, K. L. Marques and J. L. Santos, Application of quantum dots as analytical tools in automated chemical analysis: a review, ***Anal. Chim. Acta***, 2012, **735**, 9-22.
35. C. Guo, H. Zeng, X. Ding, D. He, J. Li, R. Yang and L. Qu, Enhanced chemiluminescence of the luminol-$K_3Fe(CN)_6$ system by ZnSe quantum dots and its application, ***J. Lumin***, 2013, **134**, 888-892.
36. A. Patterson, The Scherrer formula for X-ray particle size determination, ***Phys. Rev***, 1939, **56**, 978.
37. A. Khataee, R. Lotfi, A. Hasanzadeh, M. Iranifam, M. Zarei and S. W. Joo, Comparison of two methods for selegiline determination: A flow-injection chemiluminescence method using cadmium sulfide quantum dots and corona discharge ion mobility spectrometry, ***Spectrochim Acta A Mol Biomol Spectrosc***, 2016, **153**, 273-280.
38. Y. Li, P. Yang, P. Wang, X. Huang and L. Wang, CdS nanocrystal induced chemiluminescence: reaction mechanism and applications, ***Nanotechnology***, 2007, **18**, 225602.
39. Z. Wang, J. Li, B. Liu, J. Hu, X. Yao and J. Li, Chemiluminescence of CdTe nanocrystals induced by direct chemical oxidation and its size-dependent and surfactant-sensitized effect, ***J. Phys. Chem. B***, 2005, **109**, 23304-23311.
40. W. W. Yu, L. Qu, W. Guo and X. Peng, Experimental determination of the extinction coefficient of CdTe, CdSe, and CdS nanocrystals, ***Chem. Mater***, 2003, **15**, 2854-2860.
41. J. Tauc, *Mater.* Optical properties and electronic structure of amorphous Ge and Si, ***Mater. Res. Bull***, 1968, **3**, 37-46.
42. Z. Wang, J. Li, B. Liu and J. Li, CdTe nanocrystals sensitized chemiluminescence and the analytical application, ***Talanta***, 2009, **77**, 1050-1056.
43. L. Xi, W. X. W. Tan, C. Boothroyd and Y. M. Lam, Understanding and controlling the growth of monodisperse CdS nanowires in solution, ***Chem. Mater***, 2008, **20**, 5444-5452.
44. Z. B. Yu, Y. P. Xie, G. Liu, G. Q. M. Lu, X. L. Ma and H.-M. Cheng, Self-assembled CdS/Au/ZnO heterostructure induced by surface polar charges for efficient photocatalytic hydrogen evolution, ***J. Mater. Chem. A***, 2013, **1**, 2773-2776.
45. A. A. Aghuy, M. Zakeri, M. Moayed and M. Mazinani, Effect of grain size on pitting corrosion of 304L austenitic stainless steel, ***Corros. Sci***, 2015, **94**, 368-376.
46. B. Ayoubi Feiz, S. Aber, A. Khataee and E. Alipour, Electrosorption and photocatalytic one-stage combined process using a new type of nanosized TiO_2/activated charcoal plate electrode, ***Environ. Sci. Pollut. Res. Int***, 2014, **21**, 8555-8564.
47. A. Ghasemi and M. Mousavinia, Structural and magnetic evaluation of substituted $NiZnFe_2O_4$ particles synthesized

by conventional sol–gel method, ***Ceram. Int***, 2014, **40**, 2825-2834.

48. M. Koneswaran and R. Narayanaswamy, L-Cysteine-capped ZnS quantum dots based fluorescence sensor for Cu^{2+} ion, **Sens *Actuators B* Chem**, 2009, **139**, 104-109.
49. W. Zhao, Y. Fung, W. O and M. Cheung, L-cysteine-capped CdTe quantum dots as a fluorescence probe for determination of cardiolipin, ***Anal. Sci***, 2010, **26**, 879-884.
50. J. L. Adcock, N. W. Barnett, C. J. Barrow and P. S. Francis, Advances in the use of acidic potassium permanganate as a chemiluminescence reagent: a review, ***Anal. Chim. Acta***, 2014, **807**, 9-28.
51. G. Wei, C. Wei, G. Dang, H. Yao and H. Li, Determination of puerarin in pharmaceutical injection by flow injection analysis with acidic potassium permanganate–glyoxal chemiluminescence detection, ***Anal. lett***, 2007, **40**, 2179-2191.
52. G. Zhang, Y. Tang, H. Li, H. Yu and S. Sun, Chemiluminescence of potassium Permanganate–glyoxal–sulfur contained compound system, ***Anal. Lett***, 2009, **42**, 440-459.
53. H. Chen, R. Li, L. Lin, G. Guo and J.-M. Lin, Determination of l-ascorbic acid in human serum by chemiluminescence based on hydrogen peroxide–sodium hydrogen carbonate–CdSe/CdS quantum dots system, ***Talanta***, 2010, **81**, 1688-1696.
54. M. Jaky and J. Szammer, Oxidation of aldehydes with permanganate in acidic and alkaline media, Journal of physical organic chemistry, ***J. Phys. Org. Chem***, 1997, **10**, 420-426.
55. J. L. Manzoori, M. Amjadi and J. Hassanzadeh, Enhancement of the chemiluminescence of permanganate-formaldehyde system by gold/silver nanoalloys and its application to trace determination of melamine, ***Microchim. Acta***, 2011, **175**, 47-54.
56. A. Sproul and M. Green, Improved value for the silicon intrinsic carrier concentration from 275 to 375 K, ***J. Appl. Phys***, 1991, **70**, 846-854.
57. S. Belman, The fluorimetric determination of formaldehyde, ***Anal. Chim. Acta***, 1963, **29**, 120-126.

Graphical abstract

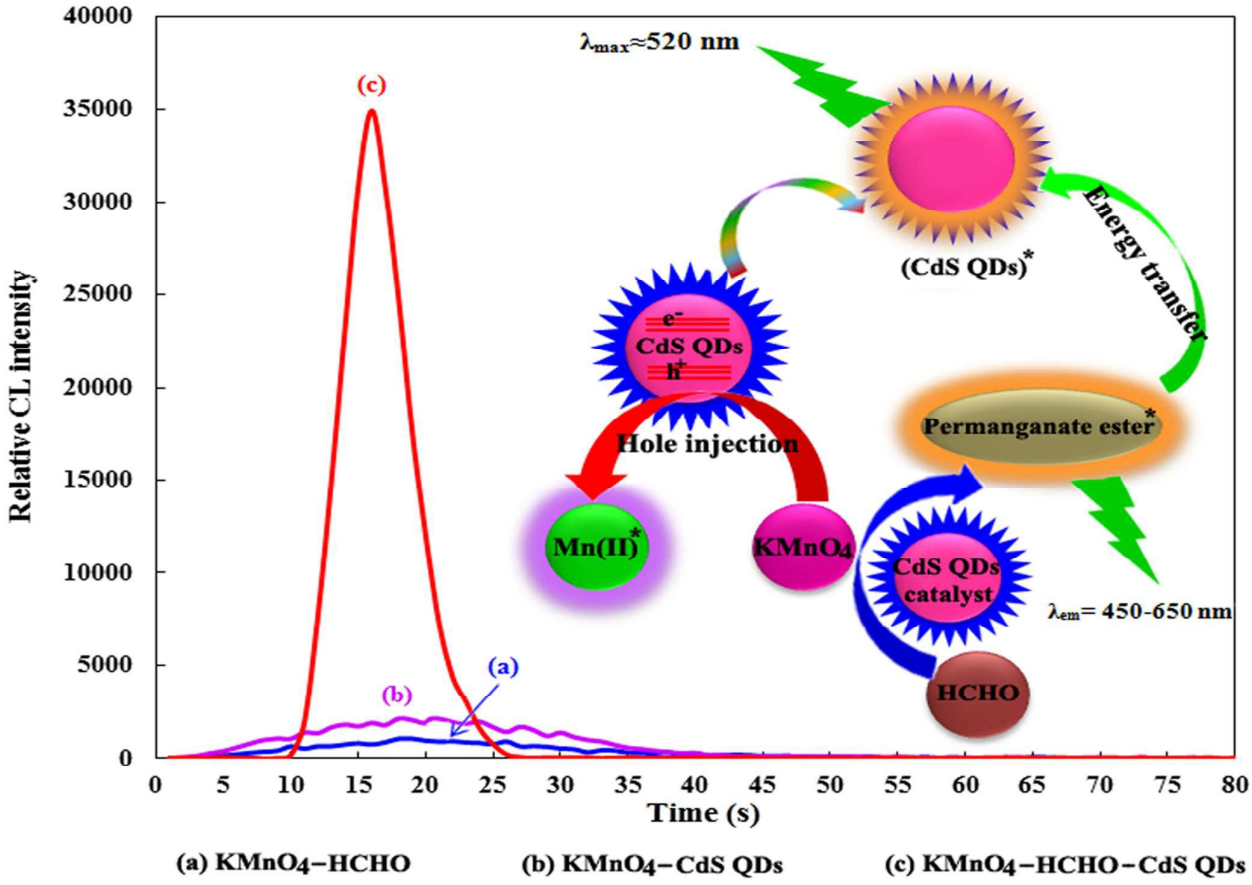

The addition of CdS QDs into $KMnO_4$−HCHO system can induce a great increase in CL signals. Furthermore, CL intensity of the $KMnO_4$–HCHO–CdS QDs system enhances by increase in HCHO concentration. The increase in the CL intensity of the $KMnO_4$–HCHO–CdS QDs system is linearly proportional to the concentration of HCHO.